

**Thermal Decomposition Studies of 1,3,3-Trinitroazetidine (TNAZ) and  
1-nitroso-3,3-dinitroazetidine (NDNAZ) by Simultaneous Thermogravimetric  
Modulated Beam Mass Spectroscopy**

Richard Behrens, Jr.<sup>‡</sup>  
Combustion Research Facility, Sandia National Laboratories  
Livermore, CA 94551

**RECEIVED**

NOV 22 1995

Suryanarayana Bulusu\*  
U.S. Army Armament Research, Development, and Engineering Center (ARDEC)  
Picatinny Arsenal, NJ 07806-5000

**OSTI**

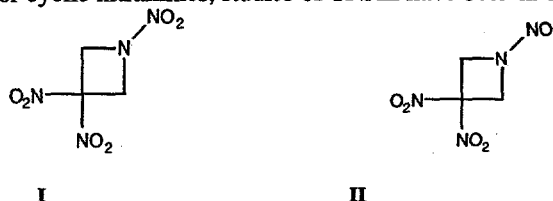
**ABSTRACT**

The initial results from a study of the thermal decomposition of TNAZ, TNAZ-1-<sup>15</sup>NO<sub>2</sub> and NDNAZ using the simultaneous thermogravimetric modulated beam mass spectrometer (STMBMS) are presented. The major products formed in the decomposition of TNAZ are NO<sub>2</sub> and NO with slightly lesser amounts of H<sub>2</sub>O, HCN, CO/N<sub>2</sub>, CO<sub>2</sub>/N<sub>2</sub>O and NDNAZ. The major product formed in the decomposition of NDNAZ is NO with lesser amounts of H<sub>2</sub>O, HCN, CO/N<sub>2</sub> and CO<sub>2</sub>/N<sub>2</sub>O. The lower molecular weight products are similar to those observed in RSFTIR and IRMPD studies conducted previously by others. However, this study has shown that the mononitroso analogue of TNAZ, NDNAZ, is an important intermediate formed during the decomposition of TNAZ. It plays an important role in determining the identity of the products formed in the decomposition of TNAZ.

The temporal behaviors of the ion signals associated with the various thermal decomposition products from TNAZ, TNAZ-1-<sup>15</sup>NO<sub>2</sub> and NDNAZ are also presented. They illustrate the evolution sequence of the various products that are associated with the different reaction pathways that control the decomposition of these materials. In particular, the study of the <sup>15</sup>N-labeled sample revealed that NO<sub>2</sub> originates from both the likely sites in the TNAZ molecule and that the cleavage of the nitramine-NO<sub>2</sub> group precedes that of the C-NO<sub>2</sub> cleavage, resulting in similar sequences in the formation of NO and NDNAZ also.

**INTRODUCTION**

TNAZ (1,3,3-trinitroazetidine) (I) and mixtures of TNAZ and NDNAZ (1-nitroso-3,3-dinitroazetidine) (II) are a relatively new energetic materials that have high energy contents and low melting points (101 and 82 C, respectively) and are being considered as a replacements for HMX and TNT. Understanding the thermal decomposition reactions of these materials is important for developing models of their combustive behavior and their response in abnormal environments. Compared to thermal decomposition studies of more conventional energetic materials, such as nitrate esters or cyclic nitramines, studies of TNAZ have been limited.



Approved for public release; distribution unlimited.

<sup>‡</sup> Research supported in part by the U.S. Army Research Office and the U.S. Department of Energy under Contract No. DE-AC0494AL85000.

\*Work supported by the U. S. Army, ARDEC.

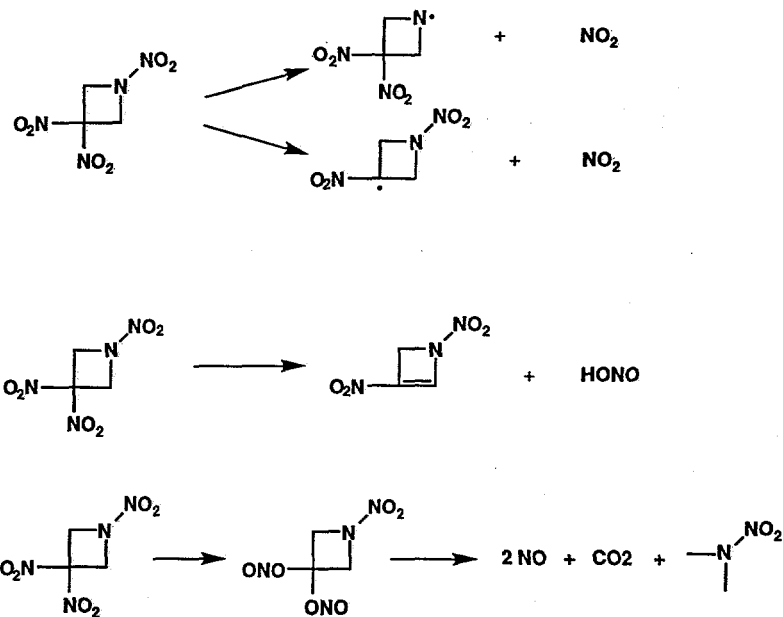
Two previous studies of TNAZ have utilized rapid-scan Fourier transform infrared (RSFTIR)<sup>1</sup> technique in the condensed phase and infrared multiphoton dissociation (IRMPD)<sup>2</sup> measurements in the gas phase to probe the decomposition processes. Based on identification of lower molecular weight products (i.e., NO<sub>2</sub>, HONO, NO) the following mechanism was proposed for the decomposition of TNAZ in the RSFTIR experiments.

One uncertainty in this mechanism centers on whether the NO<sub>2</sub> evolves from the nitramine functionality, the *gem*-dinitro functionality, or both. Another uncertainty centers on whether the nitro-nitrite rearrangement occurs as postulated in the condensed phase decomposition.

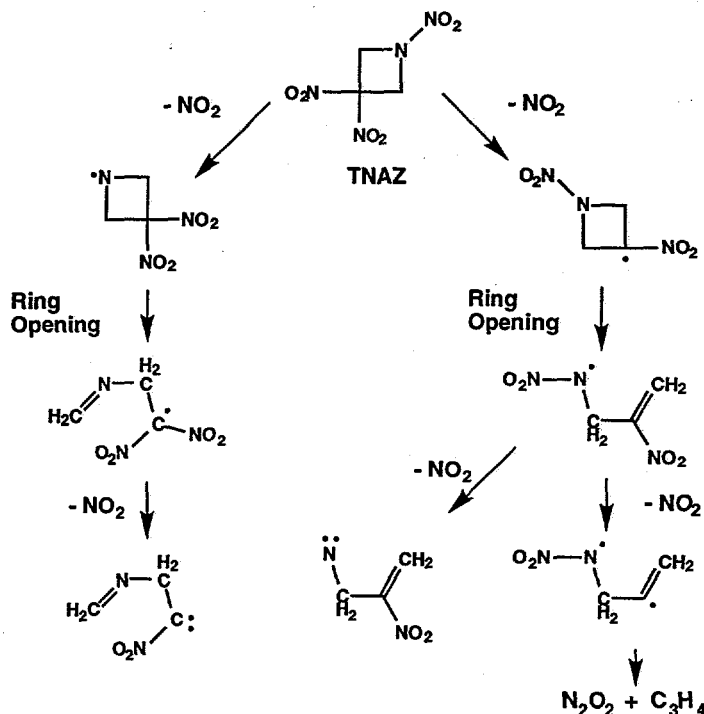
In the unimolecular decomposition of TNAZ in the molecular beam IRMPD experiments, the results obtained led to the proposal of the following mechanism.

In these experiments the initial step is the loss of NO<sub>2</sub>, followed by opening of the ring, subsequent loss of another NO<sub>2</sub> group and then fragmentation of the ring into N<sub>2</sub>O<sub>2</sub> and C<sub>3</sub>H<sub>4</sub>. Similar to the RSFTIR measurements, there is still an uncertainty as to whether the original NO<sub>2</sub> loss is from the nitramine or *gem*-dinitro group. However, the loss of NO<sub>2</sub> in the unimolecular decomposition process is clear from these results.

To develop a reasonable model to characterize the combustive behavior of TNAZ it is necessary to characterize the global reaction processes that control its decomposition behavior. In other words, is the first order process as characterized by the results from the IRMPD the rate limiting process in a higher pressure environment also, or must bimolecular processes be included to account for other reaction pathways?. For example, from the RSFTIR measurements, the appearance of HONO suggests that there is another



RSFTIR TNAZ reaction mechanism.



IRMPD TNAZ reaction mechanism.

pathway besides the C-NO<sub>2</sub> or N-NO<sub>2</sub> bond scission. In addition, our previous work on three cyclic nitramines (i.e., RDX<sup>3</sup>, HMX<sup>4</sup> and 1,3,5-trinitro-1,3,5-triazacycloheptane (TNCHP)<sup>5</sup>) suggests that formation of the mononitroso analogue of these compounds plays an important role in the decomposition of nitramines. A similar process may be occurring in the decomposition of TNAZ, namely the formation of NDNAZ.

In this paper we present results on the decomposition of TNAZ and NDNAZ from STMBMS measurements that address issues associated with the reaction mechanism that controls the decomposition of TNAZ and NDNAZ. In addition, we present the results of the decomposition study of TNAZ-1-<sup>15</sup>NO<sub>2</sub>. The quantitative gas formation rates of the decomposition products and the associated reaction kinetics will be published at a later time.

## EXPERIMENTAL

### INSTRUMENT DESCRIPTION

The STMBMS apparatus and basic data analysis procedure have been described previously.<sup>6,7</sup> This instrument allows the concentration and rate of formation of each gas-phase species in a reaction cell to be measured as a function of time by correlating the ion signals at different m/z values measured with a mass spectrometer with the force measured by a microbalance at any instant. In the experimental procedure, a small sample (~10 mg) is placed in an alumina reaction cell that is then mounted on a thermocouple probe that is seated in a microbalance. The reaction cell is enclosed in a high vacuum environment (< 10<sup>-6</sup> torr) and is radiatively heated by a bifilar-wound tungsten wire on an alumina tube. The molecules from the gaseous mixture in the reaction cell exit through a small diameter orifice (2.5 to 970 $\mu$  in these experiments, orifice length is 25 $\mu$ ) in the cap of the reaction cell, traverse two beam-defining orifices before entering the electron-bombardment ionizer of the mass spectrometer where the ions are created by collisions of 20 eV electrons with the different molecules in the gas flow. A relatively low electron energy of 20 eV (compared to 70 eV used on normal mass spectrometry measurements) is used to reduce the extent of fragmentation of the higher molecular weight ions and thus, limit their contribution to ion signals measured at lower m/z values that are associated with the thermal decomposition products. The background pressures in the vacuum chambers are sufficiently low to eliminate significant scattering between molecules from the reaction cell and background molecules in the vacuum chambers. The different m/z-value ions are selected with a quadrupole mass filter and counted with an ion counter. The gas flow is modulated with a chopping wheel and only the modulated ion signal is recorded. The containment time of gas in the reaction cell is a function of the orifice area, the free volume within the reaction cell, and the characteristics of the flow of gas through the orifice. The reaction cell used in the experiments has been described previously,<sup>7</sup> and the cap in the reaction cell is now sealed using vacuum grease and an o-ring between the taper plug and the gold foil pinhole orifice. The time constant for exhausting gas from the cell is small compared to the duration of the experiments (>~1000 sec). Note that the containment time of gas within the reaction cell is short once the gas molecules are in the free volume of the cell, but it may be much longer if the gas is trapped in the condensed-phase of the material within the cell. The pressure of the gas products within the reaction cell range from less than 1 torr for experiments with the larger diameter orifices (970 $\mu$ ) to greater than 1000 torr for experiments with the smallest diameter orifices (2.5 $\mu$ ).

### SAMPLE PREPARATION.

The TNAZ was prepared by a previously published method.<sup>8</sup> The <sup>15</sup>NO<sub>2</sub>-labeled TNAZ was prepared by treating 3,3-dinitroazetidine with H<sup>15</sup>NO<sub>3</sub>. The NDNAZ was obtained from M. Hiskey (Los Alamos National Laboratory). The samples were characterized by NMR and IR measurements. To check whether any impurity evolved from the sample, a sample is evaporated in the STMBMS apparatus prior to conducting the decomposition experiments. The results for TNAZ indicate that it is greater than 99% pure and the results for NDNAZ indicate that there is about 1 % TNAZ impurity.

### DATA ANALYSIS.

The details of the procedures for identifying the pyrolysis products by correlating the temporal behaviors of the various ion signals measured with the mass spectrometer and the analysis of time-of-flight (TOF) velocity spectra have been described previously.<sup>9</sup> In this paper we present the qualitative results of the decomposition based on the temporal behaviors of the ion signals measured with the mass spectrometer and associated with the various thermal decomposition products. Because these results are qualitative, strict comparison of the ion signal intensities from

one experiment to another can be misleading. However, quantitative results derived from these runs will be presented in a future paper.

## RESULTS AND DISCUSSION

### IDENTITY AND TEMPORAL BEHAVIOR OF THE DECOMPOSITION PRODUCTS FROM TNAZ

The two major decomposition products observed in the decomposition of TNAZ are NO (mass spec. ion signal at  $m/z=30$ ) and  $\text{NO}_2$  ( $m/z=46$ ). Other major decomposition products observed include:  $\text{H}_2\text{O}$  ( $m/z=18$ ),  $\text{HCN}$  ( $m/z=27$ ),  $\text{CO}/\text{N}_2$  ( $m/z=28$ ),  $\text{CH}_3\text{CN}$  ( $m/z=41$ ), and  $\text{NDNAZ}$  ( $m/z=176$ ). Loss of TNAZ itself is monitored by tracking ( $m/z=145$ ) which is an important fragment in the mass spectrum of TNAZ (Table 1). Smaller ion signals are observed at a number of other  $m/z$  values which will be described in a later publication. The temporal behaviors of both the thermogravimetric analysis (TGA) data and the ion signals representing these major products of TNAZ heated at  $15\text{ C}/\text{min}$ . in a reaction cell with a  $2.5\mu$  diameter orifice, are shown in Figure 1. A close examination of the data illustrates the processes that occur during the decomposition of TNAZ. First, TNAZ starts to evolve in significant quantities from the reaction cell at approximately  $150\text{ C}$  as can be seen from the sample weight and the ion signal associated with TNAZ. Even though TNAZ has a relatively high vapor pressure for an energetic material, its rate of evolution from the cell is limited due to the small  $2.5\mu$  orifice diameter used in these experiments. The ion signal associated with TNAZ increases with temperature as its vapor pressure rises until the TNAZ in the reaction cell is depleted as shown in Fig. 1. Second, examination of the ion signal representing  $\text{NO}_2$  shows that its evolution commences at approximately  $140\text{ C}$ , reaches a peak at  $230\text{ C}$  and then decreases. This behavior is consistent with a

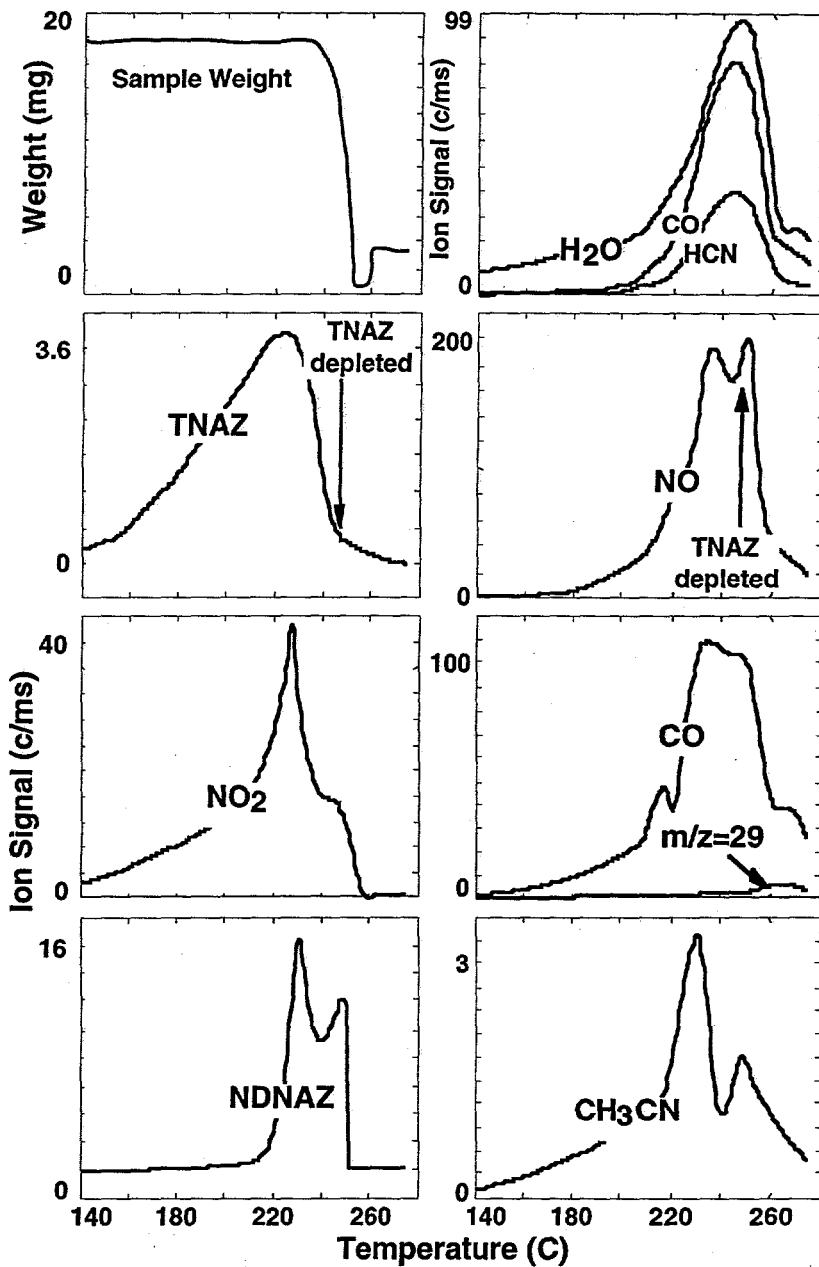


Figure 1. Ion signals representing the major decomposition products from TNAZ. The ion signals have been corrected for the evaporation of TNAZ. The  $m/z$  values representing each product are: TNAZ (145), NDNAZ (176),  $\text{NO}_2$  (46),  $\text{CO}_2/\text{N}_2\text{O}$  (44), NO (30),  $\text{CO}/\text{N}_2$  (28),  $\text{HCN}$  (27),  $\text{CH}_3\text{CN}$  (41). Orifice diameter =  $2.5\mu$ , heating rate =  $15\text{ C}/\text{min}$ .

reaction that is first order in TNAZ because the rate of decomposition of TNAZ to NO<sub>2</sub> increases with temperature and then decreases as the amount of TNAZ in the reaction cell decreases. This behavior also indicates that TNAZ is decomposing in both the liquid and gas phases since the rate of NO<sub>2</sub> formation is proportional to the total amount of TNAZ in the cell and not just the amount of TNAZ in the gas phase (which continues to increase until it nears depletion). Third, the evolution of the signals at m/z values 44 (CO<sub>2</sub>), 176(NDNAZ), 30(NO), 28(CO or N<sub>2</sub>), 27(HCN) and 41(CH<sub>3</sub>CN) continues beyond the temperatures (and times) corresponding to the evolution of NO<sub>2</sub> and also TNAZ itself. This indicates that another reaction pathway competes with the direct decomposition of TNAZ to NO<sub>2</sub> and other low molecular weight gas phase products, as observed in the RSFTIR and IRMPD experiments.

Table I. Mass spectra of TNAZ and NDNAZ\*

TNAZ		NDNAZ	
Mass	Rel. Intensity	Mass	Rel. Intensity
28	2.1%	27	1.5%
30	4.2%	28	2.9%
41	7.0%	30	50.2%
42	0.6%	41	1.4%
46	54.5%	46	0.7%
53	1.0%	53	0.6%
68	0.7%	54	0.8%
99	6.5%	129	0.6%
100	1.4%	130	5.5%
116	1.1%	176	29.3%
145	9.9%	177	1.5%
146	6.8%		

\* Mass spectra recorded using electron energy of 20 eV.

The formation of the mononitroso analogue of TNAZ, namely NDNAZ, in the decomposition of TNAZ appears to be the other major reaction pathway as will be shown in the following discussions. Formation of the nitrosamine (N-NO) from the nitramine (N-NO<sub>2</sub>) group is shown to play an important role in controlling the decomposition pathway similar to the other cyclic nitramines (i.e., RDX, HMX and TNCHP). Decomposition through the mononitroso intermediate is consistent with several of the features of the data shown in Fig. 1. For example, NDNAZ first appears at about 200 C and increases as the amount of NO increases, suggesting that NO reacts with TNAZ to form NDNAZ. The fact that the NDNAZ signal decreases as the amount of TNAZ decreases is also consistent with a direct reaction with NO. The increase in the NDNAZ signal as the TNAZ in the cell nears depletion is consistent with an increasing mole fraction of NDNAZ in the liquid phase and the resulting increase in its partial pressure in the reaction cell. Finally, evolution of CO<sub>2</sub>/N<sub>2</sub>O, NO, HCN and CO/N<sub>2</sub> after the depletion of TNAZ suggests that they are thermal decomposition products from NDNAZ.

## DISCLAIMER

This report was prepared as an account of work sponsored by an agency of the United States Government. Neither the United States Government nor any agency thereof, nor any of their employees, makes any warranty, express or implied, or assumes any legal liability or responsibility for the accuracy, completeness, or usefulness of any information, apparatus, product, or process disclosed, or represents that its use would not infringe privately owned rights. Reference herein to any specific commercial product, process, or service by trade name, trademark, manufacturer, or otherwise does not necessarily constitute or imply its endorsement, recommendation, or favoring by the United States Government or any agency thereof. The views and opinions of authors expressed herein do not necessarily state or reflect those of the United States Government or any agency thereof.

The results from an isothermal decomposition experiment with TNAZ also support a reaction mechanism consisting of parallel reaction pathways. These results at 230 C are shown in Fig. 2. NO<sub>2</sub> is an abundant decomposition product and its rate of formation falls as the amount of TNAZ falls. However, the ion signal associated with NO<sub>2</sub> (m/z=46) does not fall as rapidly as the ion signals associated with H<sub>2</sub>O and HCN. This suggests that H<sub>2</sub>O and HCN originate from reactions associated with a decomposition reaction that is first order in the total TNAZ in the reaction cell(both phases), whereas, NO<sub>2</sub> may originate from more than one source. The formation of NDNAZ from TNAZ is also clearly illustrated in Fig. 2. First an increase in the rate of formation of NO<sub>2</sub> is observed, followed by a rise in the rate of formation of NO and finally a rise in the rate of formation of NDNAZ. This is reminiscent of the RDX decomposition<sup>3</sup> in which NO<sub>2</sub> is replaced by NO to form the nitrosamine, ONDNTA. The behavior of NO<sub>2</sub>, NO and NDNAZ from TNAZ is therefore, consistent with a mechanism analogous to the one that gives ONDNTA from RDX. This suggests that the nitramine NO<sub>2</sub> group is replaced by NO in TNAZ also to form the nitrosamine analogue, as in the case of RDX.

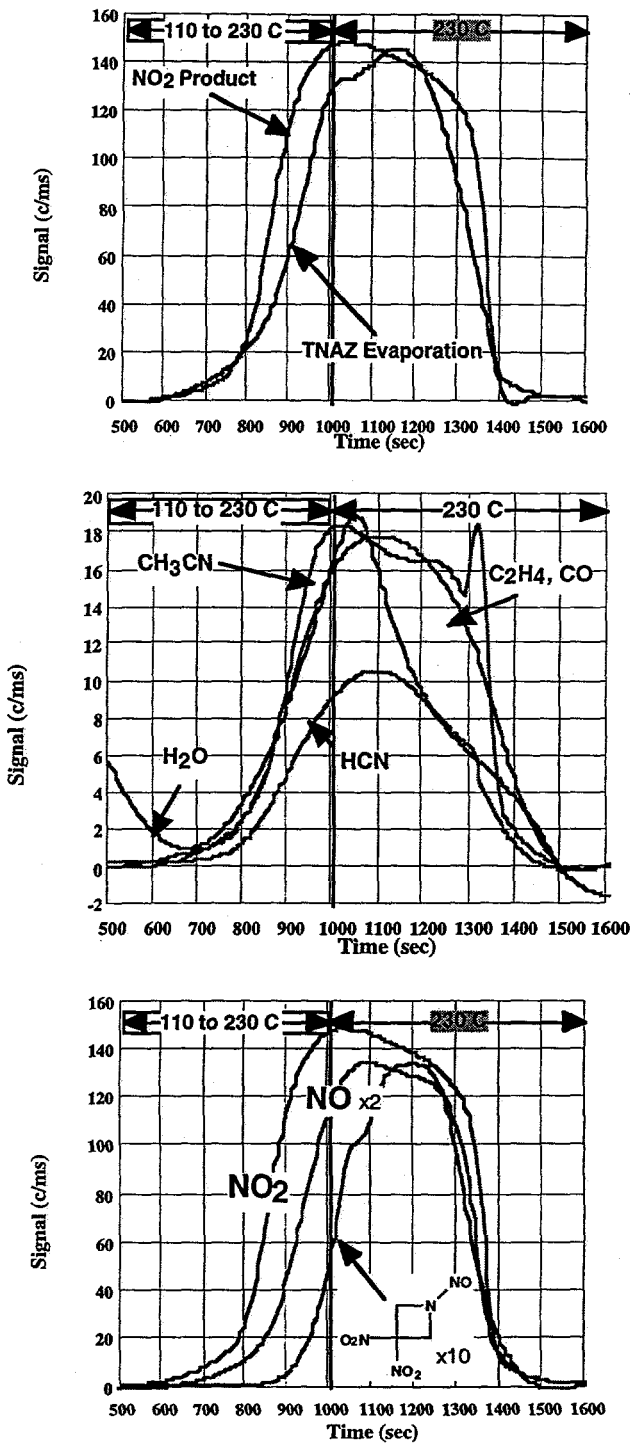


Figure 2. Ion signals representing thermal decomposition products formed from TNAZ heated to 230 C at 15 C/min and held there in the reaction cell with a 2.5 $\mu$  diameter orifice. The m/z values representing each product are: TNAZ (145), NDNAZ (176), NO<sub>2</sub> (46), NO (30), CO/N<sub>2</sub>/C<sub>2</sub>H<sub>4</sub> (28), HCN (27), CH<sub>3</sub>CN (41). The ion signals have been corrected for the contribution of signal from evaporating TNAZ.

THERMAL DECOMPOSITION  
OF TNAZ-1- $^{15}\text{NO}_2$

Figure 3 presents the ion signals obtained from the decomposition of TNAZ-1- $^{15}\text{NO}_2$  heated at 15°C/min. The most interesting differences between these signals and those from unlabeled TNAZ (Figure 1) are first, the appearance of both  $^{15}\text{NO}_2$  and  $\text{NO}_2$  signals which are of nearly equal intensities and uncorrelated. Likewise, there are separate signals each for  $^{15}\text{NO}$  /  $\text{NO}$  and  $^{15}\text{N-NDNAZ} / \text{NDNAZ}$ , also uncorrelated and of equal intensities. This clearly suggests that  $\text{NO}_2$  is formed from both the possible sites in the TNAZ molecule, namely, the nitramine group and the gem-dinitro group, but the former precedes the other significantly earlier. However, the time lags between the  $^{15}\text{N-labeled}$  and unlabeled species of  $\text{NO}$  and  $\text{NDNAZ}$  are much smaller than for  $\text{NO}_2$ . The thermal decomposition product,  $m/z = 145$  (193-48) presumably derives from elimination of  $\text{H}^{15}\text{NO}_2$  exclusively from the nitramine function and an adjacent H but not from the  $\text{C-NO}_2$  function analogous to the previous nitramines studied. The earlier conclusion that the nitroso-DNAZ is derived by a reattachment of  $^{15}\text{NO}$  or  $\text{NO}$  to the initial radical produced by the loss of nitramine- $\text{NO}_2$  is borne out by the correlations of  $^{15}\text{NO} / \text{NO}$  and  $^{15}\text{N-NDNAZ} / \text{NDNAZ}$ .

It is apparent from an examination of the  $^{15}\text{N}$  and unlabeled species shown in the plots of Figure 3 that  $\text{NO}_2$  originates from both the possible sites in the TNAZ molecule and that the cleavage of the nitramine- $\text{NO}_2$  precedes that of the  $\text{C-NO}_2$  cleavage. This also results in similar sequences of  $^{15}\text{NO} / \text{NO}$  and  $^{15}\text{N-NDNAZ} / \text{NDNAZ}$ . This observation is consistent with the fact that  $\text{N-NO}_2$  bond is weaker than  $\text{C-NO}_2$  bond. Once an  $\text{N-NO}_2$  bond cleaves other  $\text{C-NO}_2$  bonds can cleave more readily as predicted by the calculations of Melius.<sup>10</sup> It is also worth noting that the lack  $^{15}\text{N}$ -isotopic shifts shows that  $m/z$  44 and  $m/z$  28 are predominantly  $\text{CO}_2$  and  $\text{CO}$ , respectively and not  $\text{N}_2\text{O}$  and  $\text{N}_2$ .

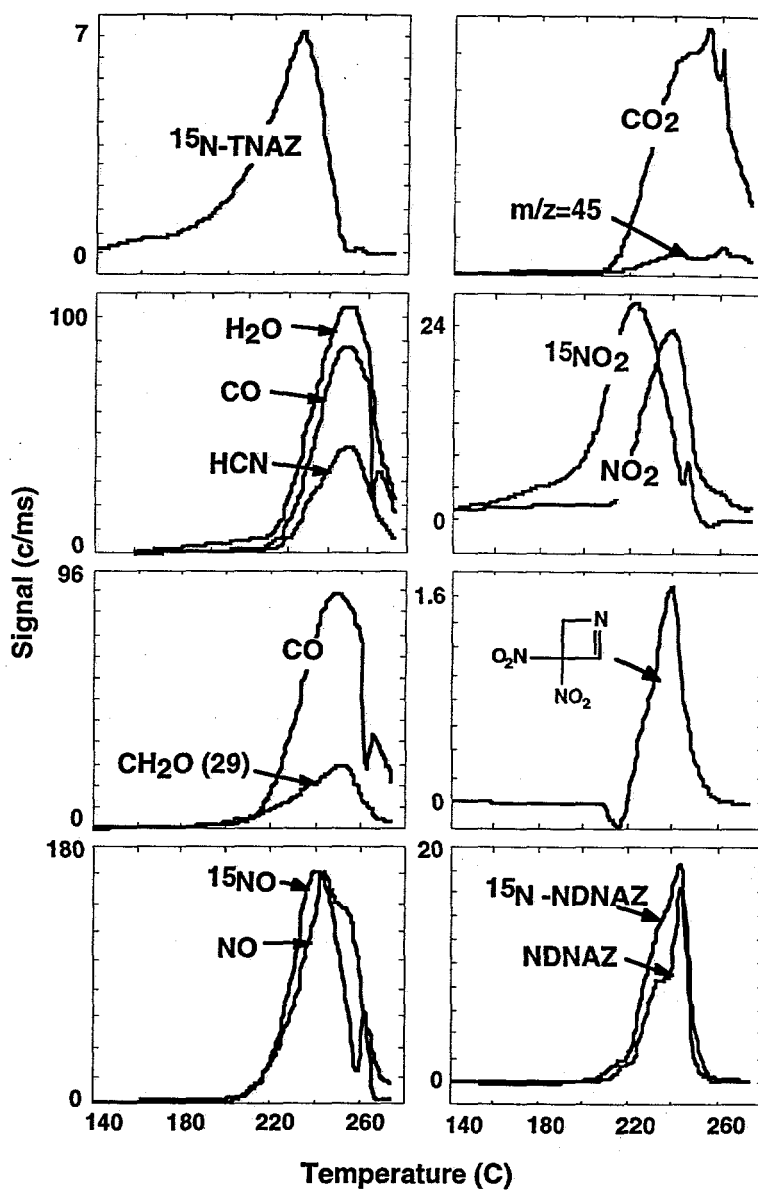


Figure 3. Ion signals representing the thermal decomposition products formed from TNAZ-1- $^{15}\text{NO}_2$  heated at 15°C/min, in a reaction cell with  $2.5\mu$  diameter orifice. The products and their  $m/z$  values are :  $\text{H}_2\text{O}(18)$ ,  $\text{HCN}(27)$ ,  $\text{CO}(28)$   $\text{CH}_2\text{O}(29)$ ,  $\text{NO}(30)$ ,  $^{15}\text{NO}(31)$ ,  $\text{CO}_2(44)$ ,  $^{15}\text{NNO} / \text{HCONH}_2(45)$ ,  $\text{NO}_2(46)$ ,  $^{15}\text{NO}_2(47)$ ,  $\text{C}_3\text{H}_3\text{N}_3\text{O}_4(145)$ ,  $\text{C}_3\text{H}_4\text{N}_4\text{O}_5(176)$  and  $\text{C}_3\text{H}_4^{15}\text{NN}_3\text{O}_5(177)$ . The ion signals have been corrected for the contribution of signals from evaporating TNAZ- 1- $^{15}\text{NO}_2$ .

## THERMAL DECOMPOSITION OF INDEPENDENTLY SYNTHESIZED NDNAZ

The thermal decomposition of NDNAZ is controlled by a complex process that forms both gas-phase and liquid-phase products. Ion signals associated with thermal decomposition products formed from NDNAZ are shown in Fig. 4 for a 12 mg sample of NDNAZ heated at 15 C/min. in a reaction cell with a  $2.5\mu$  diameter orifice.

The vapor pressure of NDNAZ is relatively high as can be seen from the large ion signal associated with the evaporation of NDNAZ in Fig. 4. The NDNAZ in this experiment is depleted when the sample reaches a temperature of  $\sim 235$  C. Examination of the ion signals associated with the thermal decomposition products shows continued evolution from the reaction cell after the NDNAZ is depleted. This suggests that products with low volatility are formed in liquid-phase during the decomposition and their evolution and decomposition continues as the sample is heated further.

NDNAZ decomposes at significant rates in these experiments starting at approximately 160 C as indicated by the first appearance of the ion signals associated with the thermal decomposition products. The rates of formation of several of the lower molecular weight gaseous products, such as CO/N<sub>2</sub> and HCN, fall to zero as the NDNAZ sample is depleted indicating that they are formed directly from the decomposition of NDNAZ. In contrast, some products start to evolve at a higher temperature and also fall off as the NDNAZ is depleted. For example, a product associated with ion signals at m/z values of 66, 67 and 68 starts to appear at approximately 180 C and its rate of formation increases rapidly at  $\sim 210$  C. Furthermore, other products start to evolve at a higher temperature and continue to evolve after the NDNAZ is depleted. Examples of this behavior can be seen with the CO<sub>2</sub>/N<sub>2</sub>O signal and ion signals representing a number of different products at m/z values of 43, 83, 99 and 128. In the case of the product represented by the m/z=128 signal the rate increases significantly after the NDNAZ is gone.

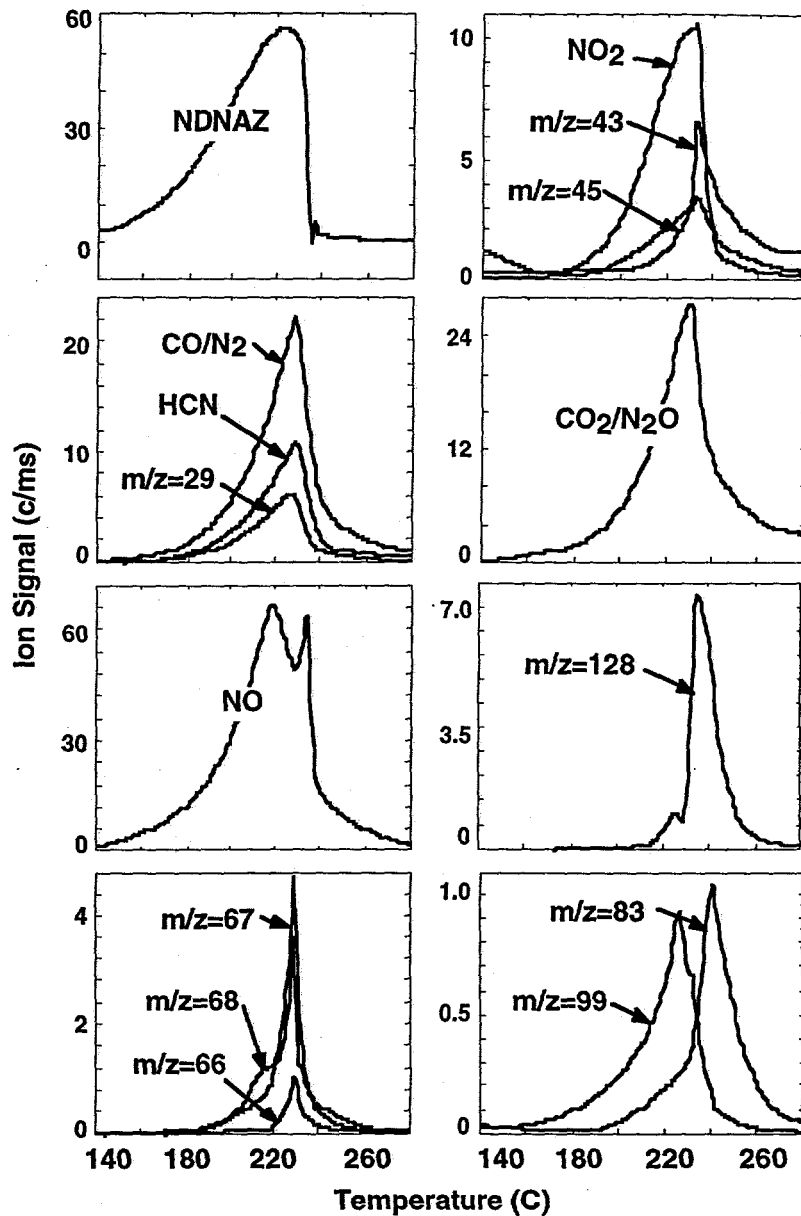


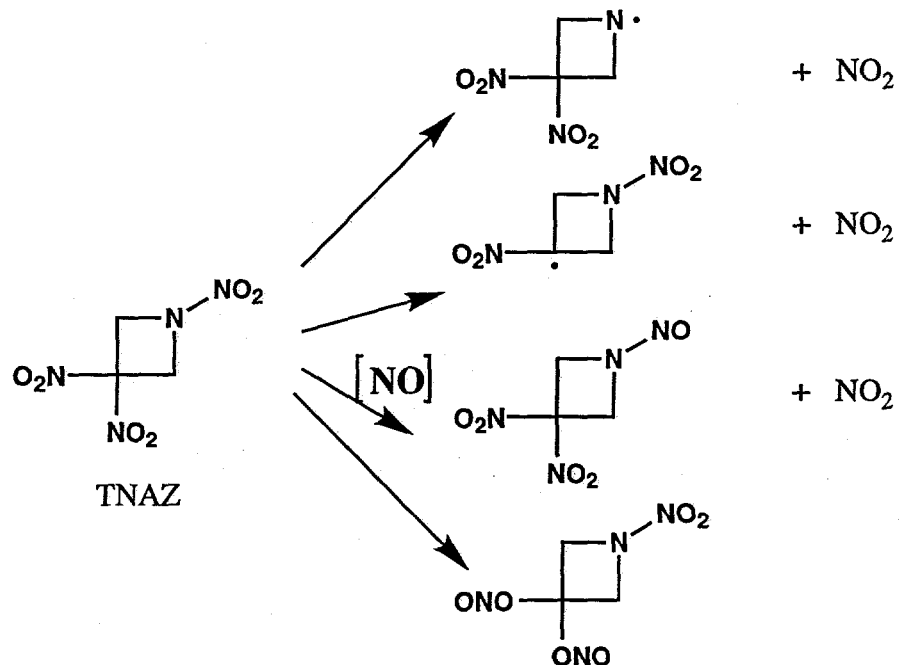
Figure 4. Ion signals representing the major decomposition products from NDNAZ. The ion signals have been corrected for the evaporation of NDNAZ. The m/z values representing each product are: NDNAZ (176), HCN (27), CO/N<sub>2</sub> (28), NO (30), NO<sub>2</sub> (46), CO<sub>2</sub>/N<sub>2</sub>O (44). Ion signals associated with pathways for TNAZ with other decomposition products are also shown. Reaction cell orifice diameter =  $2.5\mu$ , heating rate = 15 C/min.

The identities of the thermal decomposition products from NDNAZ are similar to those formed in the decomposition of TNAZ. However, the relative amounts of the major products differ significantly. For NDNAZ the major decomposition product is NO, whereas, for TNAZ both NO<sub>2</sub> and NO were the most abundant products. The next most abundant thermal decomposition products from NDNAZ are H<sub>2</sub>O, HCN, CO/N<sub>2</sub>, CO<sub>2</sub>, NO<sub>2</sub> and some of the less volatile products that remain in the liquid phase, parallel to the behavior of TNAZ. The identities of the thermal decomposition products associated with the ion signals associated with various m/z values shown in Fig. 4 require conducting TOF velocity spectra measurements which will be done in the future.

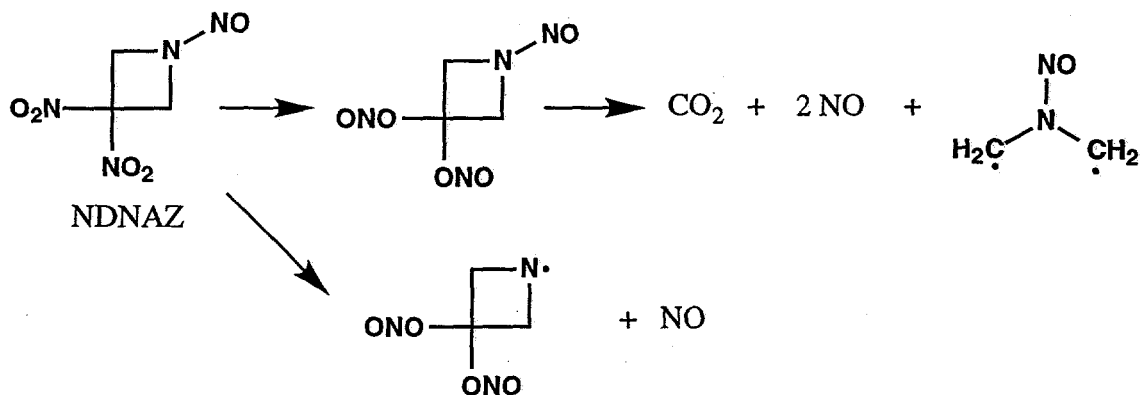
#### BASIC REACTION PATHWAYS FOR TNAZ

From the STMBMS measurements on TNAZ we have observed products that are consistent with the direct decomposition mechanisms proposed based on previous RSFTIR measurements<sup>1</sup> and unimolecular IRMPD measurements<sup>2</sup> and, in addition, we observe the new reaction product, NDNAZ, that shows that reaction pathways other than unimolecular decomposition alone must be considered in developing a mechanism for the thermal decomposition of TNAZ.

The first steps in the decomposition of TNAZ appear to be N-NO<sub>2</sub> and C-NO<sub>2</sub> bond homolysis, replacement of the nitramine NO<sub>2</sub> group with an NO group and the possible nitro-nitrite rearrangement of the NO<sub>2</sub> at the gem-dinitro group. These steps are summarized as follows:



The NO required for the conversion of TNAZ to NDNAZ may form through either the nitro-nitrite rearrangement reaction, a reaction of NO<sub>2</sub> with CH<sub>2</sub>O or via the loss of N<sub>2</sub>O<sub>2</sub> after the NO<sub>2</sub> loss and ring opening steps in the IRMPD mechanism. Once the nitroso analogue of TNAZ forms it alters the subsequent decomposition pathway by significantly reducing the direct decomposition to NO<sub>2</sub> and enhancing the rate of formation of NO. Two possible pathways for producing NO from NDNAZ are the following :



The fact that the rate of formation of NO compared to  $\text{NO}_2$  is significantly higher in the thermal decomposition of NDNAZ compared to TNAZ indicates that a nitro-nitrite rearrangement reaction is more likely for the nitrosamine than the nitramine. The formation of NO by scission of N-NO bond probably occurs but it cannot account for the significant increase of NO formed in the decomposition.

The ion signals observed in the decomposition of NDNAZ (Figure 4) also include several unassigned mass species in the range 66 - 128. Given the fact that there are only four possible atomic species (C, H, N, and O), one can speculate on the possible atomic compositions of these species as summarized in the following Table II.

Table II.

m/z	$\text{C}_3\text{H}_4\text{N}_4\text{O}_5$ (NDNAZ)	Composition
66	176 - 110 ( $2\text{HNO}_2 + \text{O}$ )	$\text{C}_3\text{H}_2\text{N}_2$
67	176 - 109 ( $\text{HNO}_2 + \text{NO}_2 + \text{O}$ )	$\text{C}_3\text{H}_3\text{N}_2$
68	176 - 108 ( $2\text{NO}_2 + \text{O}$ )	$\text{C}_3\text{H}_4\text{N}_2$
83	176 - 93 ( $\text{HNO}_2 + \text{NO}_2$ )	$\text{C}_3\text{H}_3\text{N}_2\text{O}$
99	176 - 77 ( $\text{HNO}_2 + \text{NO}$ )	$\text{C}_3\text{H}_3\text{N}_2\text{O}_2$
128	176 - 48 ( $\text{NO} + \text{H}_2\text{O}$ )	$\text{C}_3\text{H}_2\text{N}_3\text{O}_3$

The identities of the species in the last column will be established with the help of isotopic shifts using  $^{15}\text{N}$ -labeled material and time of flight velocity data both of which are currently being obtained.

The mass spectrometry data on the thermal decomposition of TNAZ and NDNAZ clearly shows many ion signals at different m/z values associated with products of secondary reactions. Several of the products come directly from the ring HCN (m/z=27) and  $\text{CH}_3\text{CN}$  (41). Others such as  $\text{H}_2\text{O}$  and  $\text{CO}/\text{N}_2$  come from secondary reactions of thermal decomposition products. While many other ion signals have not yet been associated with specific thermal decomposition products since further information is required to make these assignments.

It is clear from the STMBMS results that to construct a realistic mechanism to characterize the thermal decomposition process of TNAZ requires the use of several parallel reaction pathways. To construct a useful model of the decomposition process requires measuring the temperature dependent rate constants for each of these pathways.

#### FURTHER WORK

The work on the thermal decomposition of TNAZ and NDNAZ presented in this paper is the first steps of examining the decomposition of these materials with the STMBMS technique. Future work on TNAZ will include making TOF velocity spectra measurements of the various ion signals to determine the identities of the secondary products. Quantitative analysis of the data will be made to determine the gas formation rates of the different products as a function of time. Finally, the time and temperature dependence of the gas formation rates of the different products will be analyzed to determine the temperature dependence of the rate constants for the different reaction pathways.

## SUMMARY

The results presented in this paper on the decomposition of TNAZ show that its thermal decomposition is controlled by a number of different competitive and coupled reactions. The formation of NO<sub>2</sub> is consistent with either C-NO<sub>2</sub> and/or N-NO<sub>2</sub> bond homolysis and is in agreement with the pathways determined in the IRMPD experiments. This study has found that in the presence of decomposition products TNAZ will react with NO to form the nitroso analogue of TNAZ, NDNAZ. The temporal behaviors of the decomposition products show that as the amount of NDNAZ increases in the TNAZ sample, new products associated with the decomposition of NDNAZ appear and increase in their contribution to the overall decomposition of TNAZ. Thus, to adequately characterize even the first steps of the decomposition process bimolecular reactions must be included. The first decomposition products from TNAZ were observed at ~ 160 C in the STMBMS experiments and the formation of NDNAZ was first observed starting at ~ 200 C. Decomposition products associated with NDNAZ were observed after all of the TNAZ was gone suggesting that NDNAZ is thermally more stable than TNAZ.

The decomposition of NDNAZ shows that changing the N-NO<sub>2</sub> group to a N-NO group alters the decomposition process. For NDNAZ a much larger proportion of NO is formed than NO<sub>2</sub> in the decomposition process. This may be due to an enhanced propensity to undergo nitro-nitrite rearrangement that leads to the formation of NO and the elimination of CO<sub>2</sub> from the azetidine ring. This is consistent with our results. The decomposition of NDNAZ produces both volatile gaseous products and some products that remain in the liquid phase.

The temporal behaviors of the product species from the thermal decomposition of both TNAZ and NDNAZ indicate that the reactions occur in both the gas and liquid phases.

Further STMBMS experiments and analysis will be conducted to identify other reaction products, obtain more details on the reaction pathways and determine the temperature dependent rate constants for the different pathways.

## ACKNOWLEDGMENTS

We would like to acknowledge David Puckett for collecting the experimental data and to Dr. Michael Hiskey for supplying the NDNAZ.

- 1 a) Y. Oyumi and T. B. Brill, *Combust. Flame*, **62**, 225 (1985); b) Y. Oyumi and T.B. Brill, *Combust. Flame*, **68**, 209 (1987).
- 2 D. S. Anex, J.C. Allman, and Y.T. Lee, *Chemistry of Energetic Materials*, G. A. Olah, ed., Academic Press, 1991, p. 27.
- 3 a) R. Behrens, Jr. and S. Bulusu, *J. Phys. Chem.*, **96**, 8877, (1992); b) R. Behrens, Jr. and S. Bulusu, *J. Phys. Chem.*, **96**, 8891, (1992).
- 4 a) R. Behrens, Jr., *J. Phys. Chem.*, **94**, 6706, (1990); b) R. Behrens, Jr. and S. Bulusu, *J. Phys. Chem.*, **95**, 5838, (1991).
- 5 R. Behrens, Jr. and S. Bulusu, *Mat. Res. Soc. Symp. Proc.*, **296**, 13, (1993).
- 6 a) Behrens, Jr., R., *Rev. Sci. Instrum.*, **1986**, 58, 451; b) Behrens, Jr. R., "The Application of Simultaneous Thermogravimetric Modulated Beam Mass Spectrometry and Time-of-Flight Velocity Spectra Measurements to the Study of the Pyrolysis of Energetic Materials." In "Chemistry and Physics of Energetic Materials", Bulusu, S. N., Ed.; Proceedings of the NATO Advanced Study Institute, Vol. 309, Kluwer Academic Publishers, Netherlands, **1990**, p. 327.
- 7 Behrens, Jr., R., *Int. J. Chem. Kinetics*, **1990**, 22, 135.
- 8 T. G. Archibald, R. Gilardi, K. Baum, and M. C. Cohen, *J. Org. Chem.*, **55**, 2920 (1990).
- 9 Behrens, Jr., R., *Int. J. Chem. Kinetics*, **1990**, 22, 159.
10. Melius, C. F. and Binkley, J.S., In Proceedings of the 21st Symposium (International) on Combustion, 1987; The Combustion Institute: Pittsburgh, PA, 1988, p. 1953.